Pathogenesis and treatment of skeletal metastasis : studies in animal models

Buijs, J.T.

Chapter 2

Prognostic Significance of Periodic Acid-Schiff-positive Patterns in Primary Breast Cancer and its Lymph Node Metastases

Breast Cancer Res Treat 2004; 84:117-30.

Jeroen T Buijs[1]
Anne-Marie Cleton[2]
Vincent THBM Smit[2]
Clemens WGM Löwik[1]
Socrates E Papapoulos[1]
Gabri van der Pluijm

Departments of Endocrinology[1] and Pathology[2],
Leiden University Medical Center,
Leiden, The Netherlands

Abstract

Invasive ductal carcinoma is by far the largest histological subtype of breast cancer, but clinical behavior can differ greatly. Reliable morphological markers are, therefore, of invaluable help to distinguish between patients with good and poor prognosis. Histological patterns stained with periodic acid-Schiff (PAS) were previously shown to be of prognostic significance in cutaneous and uveal melanoma. In this study, we examined the presence of different PAS-positive (PAS+) structures in 54 women with infiltrating ductal adenocarcinoma of the breast and at least one axillary lymph node metastasis but no distant metastases who were followed for at least 11 years.

We found that the complexity of the thin PAS+ patterns in lymph node metastases is associated with a shorter period of disease-free survival (DFS) as well as of total survival (Kaplan Meier curves). Furthermore, the presence of PAS+ networks – the most complex thin PAS+ pattern – in lymph node metastases is one of the two independent factors associated with the occurrence of a distant metastasis (multivariate Cox model). Moreover, the presence of PAS+ networks in positive lymph nodes is the feature most strongly associated with DFS.

In conclusion, the presence of PAS+ networks in lymph node metastases is a new, reliable and convenient indicator for prognosis of breast cancer patients.

Introduction

Breast cancer is the most frequent type of cancer among women in industrialized countries. Approximately one in twelve women will develop breast cancer during their lifetime, and the incidence is increasing in many countries. Locoregional metastasis to adjacent lymph nodes is a crucial event of breast cancer progression and, consequently, axillary nodal status is the best predictor of survival [1].

During cancer progression blood supply is required for tumors to survive, grow, and metastasize [2,3]. Tumor angiogenesis, the process of blood vessel formation into a growing tumor, is necessary, as a tumor can not grow beyond 3 mm^3 in the absence of angiogenesis due to the concomitant lack of oxygen and nutrients [4-6]. Several groups have shown that high blood vessel counts in primary breast, and other, cancers provide an independent predictor of poor prognosis [7-10].

In addition to angiogenesis, evidence is accumulating that malignant tumors are often capable of inducing other structures that may contribute to (invasive) growth and dissemination. In both uveal and cutaneous melanoma the presence of networks that stain positive with periodic acid-Schiff (PAS) has been described [8,11-13] and these have been shown to be of prognostic significance [13-15]. The PAS reaction is a non-specific indicator for polysaccharides, which are present in the basement membranes, including those of blood vessels. The PAS+ patterns may represent (a mixture of): blood vessels/ vascular network [12,14], fibrovascular tissue [16,17], tumor cells [18] or a fluid conducting meshwork [11]. Hence, at present, no consensus exists about the exact nature and origin of the PAS+ pattern. In melanoma PAS+ meshworks that were most interconnected correlated with the poorest prognosis, suggesting that these structures may facilitate tumor growth and/or dissemination [13-15].

Invasive ductal carcinoma is by far the largest histological subtype of breast cancer (at least 80%), but clinical behavior can be quite different. Reliable morphological markers are, therefore, needed for distinguishing patients with good and poor prognosis. In the present study, we investigated the presence of different PAS+ patterns in the primary tumor and its lymph node metastases of women with infiltrating ductal adenocarcinoma of the breast. Our results show that the presence of these patterns has significant prognostic value for both disease-free survival and total survival.

Patients & Methods

Patients

Out of 251 women with breast cancer operated between April 1984 and November 1989 in the Leiden University Medical Center, 170 had infiltrating ductal adenocarcinomas, no distant metastases at the time of surgery, no other malignant tumors and at least one paraffin embedded tissue was available for examination. Of these, 79 had at least one positive lymph

node and were included in the study. Twenty-three patients were excluded for the following reasons: no follow-up (4), paraffin blocks of either the primary tumor or its lymph node metastases were not available (20), or paraffin blocks of the primary tumor or its lymph node metastases had such quality that tumor histology and staining could not be examined properly (1). This analysis, therefore, includes 54 patients with infiltrating ductal adenocarcinomas with at least one lymph node metastasis, but no distant metastases, in whom material from both the primary tumor and the lymph nodes was available. The excised breast carcinomas and lymph nodes were fixed with formalin and embedded in paraffin for routine histopathological examinations. All primary breast tumors were revised and graded according to Bloom and Richardson (BAR) by a pathologist (V.T.H.B.M.S.). Patients were followed periodically according to existing protocols.

Periodic Acid-Schiff (PAS)

Periodic acid-Schiff (PAS)-staining was performed on 5 μm paraffin embedded sections. Sections were deparaffinized and rehydrated in the following immersion steps: 5' Paraclear (2x)(Klinipath, Duiven, The Netherlands), 2' 100% ethanol (2x), 2' 96%, 2' 80%, 2' 70%, 2' 50% and 2' distilled water. The sections were incubated for 30 minutes in a 56 °C pre-warmed 0.6% periodic acid solution. The sections were rinsed with distilled water, and Schiff's reagent (Feulgen stain, Klinipath, Duiven, The Netherlands) was added. After 30 minutes, the sections were washed for 15 minutes with tap water. Samples were counterstained with Mayer's Hematoxylin (Merck, Amsterdam, The Netherlands) for 1 minute and washed with tap water for 10 minutes before being dehydrated and mounted in xylol under glass coverslips with Aquamount.

Immunohistochemistry

All 5 μm paraffin embedded sections were mounted on slides coated with aminopropylethoxysilane (APES) followed by glutaraldehyde. After overnight drying in an oven at 37 °C, slides were stored in slide boxes at a temperature of 4 °C, to avoid loss of antigen epitopes [19]. The sections were deparaffinized and rehydrated in the following steps: 5' Paraclear (2x) (Klinipath, Duiven, The Netherlands) and 2' 100% ethanol (2x). To block endogenous peroxide activity of the tissue, 20 minutes incubation at room temperature with 1% hydrogen peroxide in methanol was done. Microwave antigen retrieval (AR) was done for vimentin [20], in brief: sections were boiled for 10 minutes in a solution of 10 mmol/L citrate buffer pH 6 in a domestic microwave oven at full power (Electrolux 700W). Enzymatic digestion was performed with trypsin (CD31), treatment at 37 °C for 20 minutes, using 0.1% trypsin (Sigma T-8128) in 0.1% calcium chloride pH 7.4. All incubations and washing with phosphate-buffered saline were performed at room temperature. Sections were incubated with the primary antibodies overnight, followed by 30 minute incubations with biotin-labeled rabbit-anti-mouse Ig or biotin-labeled goat-anti-rabbit Ig and a preformed complex of biotin-labeled horserad-

ish peroxidase and streptavidin (DAKO). CD31 (clone JC/70A, dilution 1:200) and von Willebrand Factor (vWF)(polyclonal, dilution 1:400) were supplied by DAKO (Glostrup, Denmark), vimentin (clone V9, dilution 1:300) by Monosan (Uden, The Netherlands) and Smooth Muscle Actin (clone ASM-1, dilution 1:1000) by Progen (Heidelberg, Germany). Immune complexes were visualized with 0.05% diaminobenzidine and 0.0015% hydrogen peroxide. Slides were counterstained in Mayer's hematoxylin (Merck, Amsterdam, The Netherlands) for 30 seconds and washed with tap water for 10 minutes before being dehydrated and mounted in xylol under glass coverslips with aquamount.

Statistical Analyses

Patients were divided into two groups, according to the presence or absence of a particular PAS+ pattern. Subsequently, Kaplan-Meier curves were calculated and compared with a log-rank test for survival and disease free survival. The level of significance was set at P = 0.05. Afterward, the relative importance of all PAS+ patterns and the major clinical and prognostic characteristics (histological grade, stage, age, the number of positive lymph nodes at time of surgery and treatment of primary tumor) were determined by multivariate analysis using the Cox proportional hazards model. The Cox model was constructed using a forward stepwise selection procedure on the basis of the likelihood ratio statistic with chi-square scores with significance levels of 0.05 or less for entry, and chi-square scores with significance levels of 0.10 or greater for removal.
SPSS-10 was used for all calculations.

Results

Patients

Stage, histological grade, treatment of primary tumor, kind of adjuvant treatment, age at time of surgery, disease free survival (DFS; end-point is the occurrence of a distant metastasis) and total survival (end-point is the occurrence of cancer-related death) are summarized in table 1.

Morphological PAS-positive Patterns

Sections stained with PAS were interpreted by two investigators (J.T.B. and G.v.d.P.) and a pathologist (V.T.H.B.M.S.). Different morphological patterns were identified within the tumor (Fig. 1). A subset of the patterns in this study, the 'thin PAS-positive (PAS+) patterns' or the 'thin PAS+ meshwork' (E-J), as described by Foldberg and co-workers [12], existed within a compact tumor mass. We discerned 10 distinct PAS+ patterns in primary breast cancer and their lymph node metastases:

A. *Small curves of extra cellular matrix*: curves of PAS+ connective tissue (CT) around small groups of tumor cells (3-10 cells)(Fig. 1*A*).

Table 1 **Classification of all patients included in the study.** Stage, Histological Grade (both a.), treatment of primary tumor, adjuvant therapy (b.), age, disease freesurvival (DFS) and survival (all c.) are summarized. MRM = modified radical mastectomy, BCT = breast conserving treatment, RT = radio therapy, Horm = hormone therapy and Chem = chemotherapy , Age = age at time of surgery, St.dev = standard deviation, SEM = standard error of the mean.

(a)

	Stage				Histological Grade		
All patients	**II A**	**II B**	**III A**	**III B**	**1**	**2**	**3**
54 (100%)	7 (13.0%)	19 (35.2%)	7 (13.0%)	21 (35.5%)	4 (7.4%)	17 (27.8%)	33 (61.1%)

(b)

		Adjuvant therapy						
		None	**Chem**	**Horm**	**RT**	**RT +**	**RT +**	**Total**
Treatment of primary tumor	**MRM**	11	3	1	21	9	4	49 (90.7%)
	BCT + RT	2	2	1	x	x	x	5 (9.3%)

(c)

	Age (in years)	**DFS (in years)**	**Survival (in years)**
Average	57.83	4.63	6.58
Median	57.29	3.74	5.72
St.dev	12.09	4.19	4.13
SEM	1.54	0.53	0.52
Range	27.77 - 84.20	0.20 - 16.15	0.20 - 16.15

B. *Small cellclusters surrounded by CT*: dominant PAS+ CT network with small cluster, <10 cells, of breast cancer cells (Fig. 1*B*).

C. *Large cellclusters surrounded by CT*: dominant PAS+ CT network with clusters, ≥ 10 cells, of breast cancer cells (Fig. 1*C*).

D. *Thick circular loops of CT*: composed of thick, circular PAS+ CT layers around clusters of breast cancer cells (>20 cells)(Figure 1.d). Because of their circular shape, these thick circular loops of CT may be confused with looping patterns that form networks. However, 'thick circular loops of CT' are presented as thick, dominant layers, obviously consisting of CT. (Fig. 1*D*)

E. The *parallel* pattern: straight thin PAS+ patterns are arranged parallel to one another without dichotomous branching or cross-linking (Fig. 1*E*).

F. The *parallel with cross-link* pattern: parallel straight thin PAS+ patterns are linked to each other in a fashion reminiscent of switching tracks in a rail yard (Fig. 1*F*).

G. *Arcs*: thin PAS+ arcs are incomplete loops (i.e. loops that are not closed). We made no attempt to obtain serial sections through tumors to determine whether these arcs become complete loops in deeper section planes (Fig. 1*G*).

H. *Arcs with branching*: PAS+ arcs demonstrate dichotomous branching (Fig. 1*H*).

I. *Loops*: completely closed thin PAS+ circles. The presence of one closed loop is sufficient evidence to record this pattern as present (Fig. 1*I*).
J. *Interconnected Loops*: back-to-back closed PAS+ loops. By definition, if interconnected loops are present, loops must be present (Fig. 1*J*).

Immunohistochemical Characterization of the Thin PAS+ Patterns

Antibodies to vWF or CD31 (PECAM-1) have been frequently used to visualize the blood vessels, and antibodies to Flt-4 (VEGFR-3) have been used to visualize lymph vessels, although blood vessels in a tumor might be stained as well [21].

In this study, the expression of vWF and Flt-4 (Fig. 2) was indeed mainly restricted to (blood) vessels (overview in Table 2). CD31 was also found to be expressed on blood vessels. In addition, the different thin PAS+ patterns depicted in figure 1 stained positive for smooth muscle actin (SMA)(Fig. 3). Occasionally, lumina were found in the PAS+ patterns. Lumina stained both unilaterally and bilaterally for SMA (Fig. 3*E,F*), but were negative vWF and Flt-4. Tumor cells and, sporadically, erythrocytes were found in these lumina. The vWF+/CD31+ tumor blood vessels (Fig. 2*A,B* and 4*A*), which contained numerous erythrocytes, were located in bifurcations of this SMA+/PAS+ meshwork and might be interconnected to these lumina, suggesting an additional form of perfusion/dissemination for the tumor in the PAS+ meshwork. In summary, two different types of structures were observed in the thin PAS+ meshwork:

1. Tumor blood vessels, vWF+/CD31+.
2. "Additional meshwork", PAS+/SMA+ (vWF-negative).

Table 2 **Summary of staining of specific tissues as seen in the study.** Vessels with erythrocytes were considered as blood vessels. Specific staining for lymph vessels was not scored, since lymph vessels and blood vessels without erythrocytes can not be distinguished. VWF = von Willebrand Factor, SMA = smooth muscle actin.

Antibody	Blood Vessels	Stroma	Arcs (G+H)	Loops (I)	Networks (J)
CD 31/PECAM-1	+	-	Patchy	Patchy	Patchy
VEGFR-3 (Flt-4)	+	-	-	-	-
VWF	+	-	-	-	-
SMA	+	+	+	+	+
Vimentin	+	+	Patchy	Patchy	Patchy
Other					
PAS-staining	+	+	+	+	+

The expression of CD31 in some primary breast carcinomas and concomitant lymph node metastases appeared not exclusive for blood vessels containing a lumen ((Fig. 4*C,D*). In addition, expression of CD31 was repeatedly found as a patchy, discontinuous staining alongside parts of the PAS+/SMA+ meshwork. Patchy staining alongside the entire meshwork was found for vimentin expression as well (data not shown).

Occasionally, it was found that breast cancer cells were polarized to the meshwork, resembling the organization of normal breast ductal epithelial cells that are polarized to myoepithelial cells (Fig. 4*D*).

PAS-positive Patterns and Prognosis

The presence or absence of each morphological pattern in both primary tumor and positive lymph node was recorded for each patient with no knowledge of the clinical outcome (Table 3). The identification of thin PAS+ patterns was highly reproducible (Table 4). Various types of thin PAS+ patterns were frequently observed within the same tumor. In primary breast cancer as well as in its lymph node metastasis the incidence of thin PAS+ patterns that were most interconnected, the PAS+ networks (14.8% and 13.0%, respectively) and loops (20.4% and 18.5%, respectively), was lower than the incidence of thin PAS+ patterns that were less interconnected. In the primary tumor and its positive lymph node the presence of any thin PAS+ pattern was 29.6% and 35.2%, respectively. The presence of any thin PAS+ pattern was for 63% concordant between the primary tumor and its positive lymph node (data not shown). Apart from 'thick circular loops of CT', other PAS+ structures, which were thick and associated with CT, were scored more frequently.

Table 3 **Distribution of Morphological PAS-positive (PAS-+) Patterns in Primary Breast Carcinomas and their lymph node metastases.** In brackets is the percentage of the patients having a particular PAS+ pattern.
ECM = extracellular matrix, CT = connective tissue.

	PAS+ patterns	Primary breast carcinoma	Lymph node metastasis
ECM-rich patterns	Small curves of ECM (A)	18 (33.3%)	32 (59,3%)
	Small cellclusters surrounded by CT (B)	33 (61.1%)	17 (27.8%)
	Large cellclusters surrounded by CT (C)	34 (63.0%)	15 (27.8%)
	Thick circular loops of CT (D)	12 (22.2%)	7 (13.0%)
	Parallel (E)	10 (18.5%)	14 (25.9%)
	Parallel with Cross-Links (F)	10 (18.5%)	13 (24.1%)
Thin PAS+ patterns	Arcs (G)	12 (22.2%)	14 (25.9%)
	Arcs with Branching (H)	12 (22.2%)	13 (24.1%)
	Loops (I)	11 (20.4%)	10 (18.5%)
	Networks (J)	8 (14.8%)	7 (13.0%)
	Any thin PAS+-pattern	16 (29.6%)	19 (35.2%)
	Total number of patients	54 (100%)	

To determine which of the ten PAS+ patterns might be associated with clinical outcome, Kaplan-Meier (KM) survival curves (Fig. 5 and 6) were estimated from the data (Table 5). None of the (thin) PAS+ patterns in the primary mammary carcinoma was significantly associated with poor prognosis.

Table 4 Agreement between two independent observers for each thin PAS+ pattern.

Thin PAS+ patterns	% Agreement	Chance corrected measure of agreement (kappa statistics)
Parallel (E)	88	0.639
Parallel with Cross-Links (F)	88	0.639
Arcs (G)	85	0.677
Arcs with Branching (H)	85	0.677
Loops (I)	85	0.641
Networks (J)	88	0.693
any thin PAS+ pattern	85	0.687

Note: P ⩽ 0.001 for all observations

Table 5 Kaplan-Meier Analysis for Disease Free Survival (DFS) and Total Survival for the Presence of Morphological PAS-positive (PAS+) Patterns in Primary Breast Carcinomas and their Lymph Node Metastases. ECM =extra cellular matrix, CT = connective tissue.

		Primary breast carcinoma				Lymph node metastasis			
		Disease free survival		Total survival		Disease free survival		Total survival	
	PAS+ patterns	Log-rank X2	P	Log-rank X2	P	Log-rank X2	P	Log-rank 2	P
ECM rich patterns	Small curves of ECM (A)	0.54	0.4604	0.01	0.9302	1.18	0.2771	1.09	0.2975
	Small cellclusters surrounded by CT (B)	0.07	0.7929	< 0.01	0,9894	3.11	0,0779	5.16	0,0231
	Large cellclusters surrounded by CT (C)	0.02	0.8950	0.02	0.8950	1.10	0.2935	0.24	0,6221
	Thick circular loops of CT (D)	< 0.01	0.9791	0.01	0,9214	2.56	0,1094	11.88	0,0006
Thin PAS+ patterns	Parallel (E)	0.08	0.7808	0.05	0.8170	3.13	0.0770	0.18	0,6689
	Parallel with Cross-Links (F)	0.08	0.7808	0.05	0.8170	3.26	0,0711	0.16	0,6918
	Arcs (G)	0.02	0.8930	0.57	0.4485	8.48	0,0036	11.09	0.0009
	Arcs with Branching (H)	0.02	0.8930	0.57	0.4485	7.62	0,0058	8.92	0,0028
	Loops (I)	0.10	0.7503	0.80	0.3700	13.89	0,0002	17.49	< 0,0001
	Networks (J)	1.26	0.2620	1.06	0.3023	18.86	< 0,0001	17.02	< 0,0001
	Any thin PAS+-patterns	0.63	0.4275	0.67	0.4131	9.73	0,0018	3.00	0,083

Table 6 Cox Proportional Hazards Model Using Forward Stepwise Selection of Prognostic Factors in Breast Cancer for DFS. DF = degrees of freedom, SE = standard error.

Variable	DF	Paramater estimate	SE	Wald chi-square	P	Hazard ratio	95 % Confidence interval
PAS+ network	1	2.463	0.524	22.077	< 0.0001	8.78	3.27 - 23.60
Stage-classification	1	0.413	0.151	7.481	0.005	1.50	1.13 - 1.98

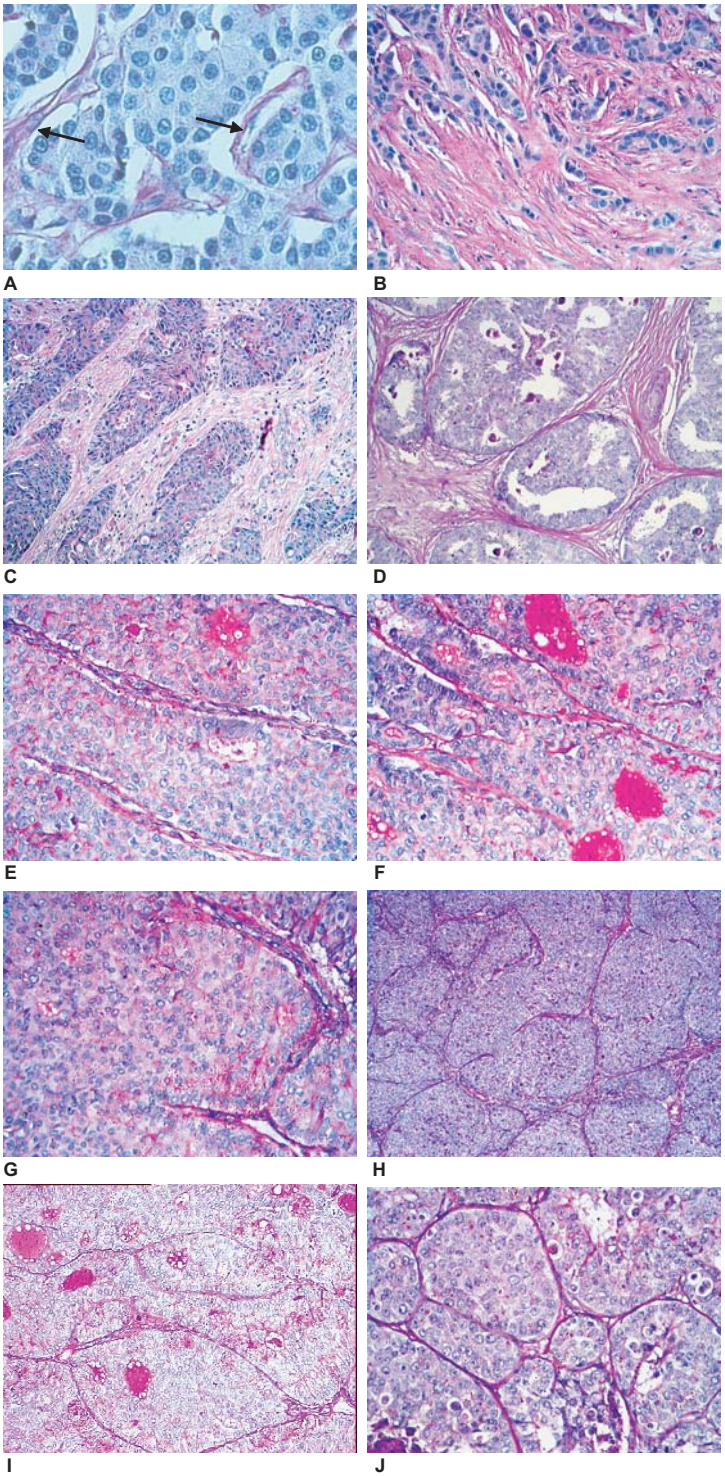
A
B
C
D
E
F
G
H
I
J

Figure 1 **(left) Primary Breast Carcinoma Could Contain a Combination of Different PAS+ Patterns.** Typical patterns are shown by an example. *A*, *small curves of ECM* with total lack of structure around small numbers of tumor cells (arrows) (magnification 400x). *B*, *small cellclusters surrounded by CT*: dominant CT network with breast cancer cells (magnification 200x). *C*, *large cellclusters surrounded by CT*: dominant PAS+ CT network with clusters of breast cancer cells (> 10 cells)(magnification 200x). *D*, *thick circular loops of CT*: thick, circular PAS+ CT layers around clusters of breast cancer cells (>30 cells) (magnification 100x). *E*, *parallel* pattern; straight vessels are arranged parallel to one another without dichotomous branching or cross-linking (magnification 400x). *F*, *parallel with cross-link* pattern: parallel straight vessel are linked to each other in a fashion reminiscent of switching tracks in a rail yard (magnification 400x). *G*, *arcs* are incomplete loops (i.e., the loops that are not closed) (magnification 400x). *H*, *arcs with branching* demonstrate dichotomous branching (magnification 100x). *I*, *loops*: completely closed. The presence of one closed loop is sufficient evidence to record this pattern as present (magnification 200x). 'Arcs with branching' are often founded in 'loops' (magnification 200x). *J*, *network*: Adjacent back-to-back closed loops forming *interconnected loops*.

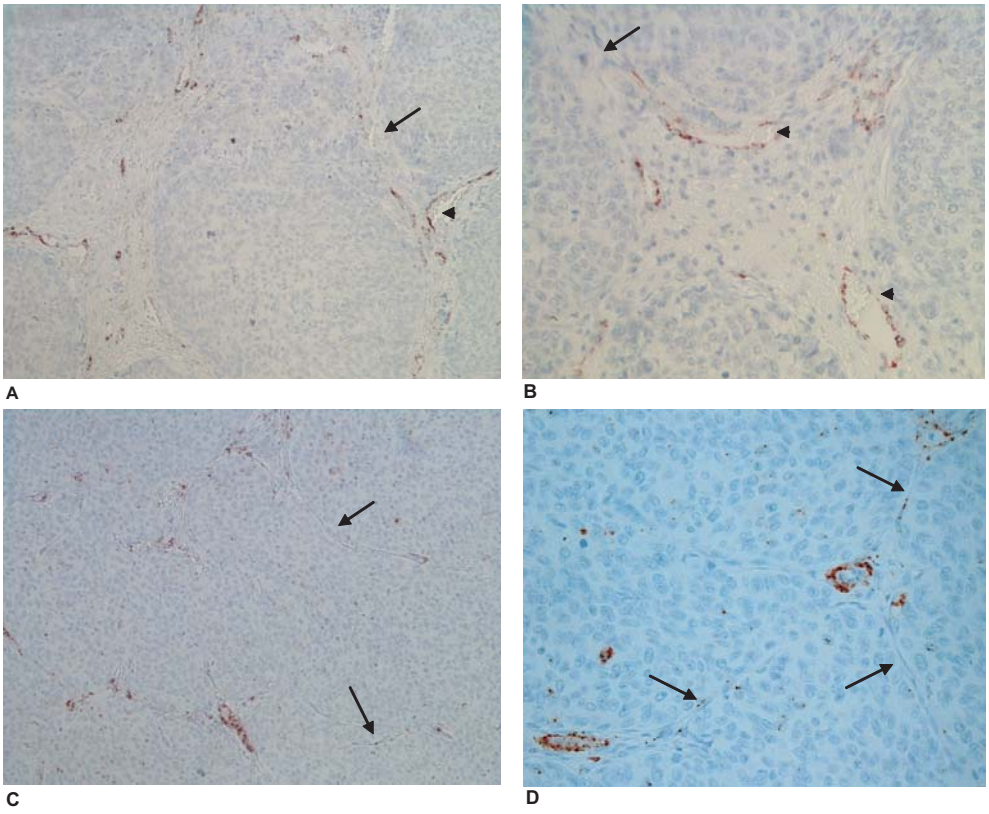

Figure 2 **Vessels in a lymph node metastasis from breast cancer.** *A*, *B*, the tumor is well vascularized as shown by the von Willebrand Factor (vWF)-positive blood vessels, which have erythrocytes inside (arrowheads). Besides the blood vessels, no additional patterns have been stained with the vWF staining (magnifications 100x and 200x, respectively). *C*, *D*, expression of Flt-4 shows staining of vessels. The additional PAS+ patterns (arrows) are not stained with Flt-4 or vWF (magnifications 100x and 200x, respectively).

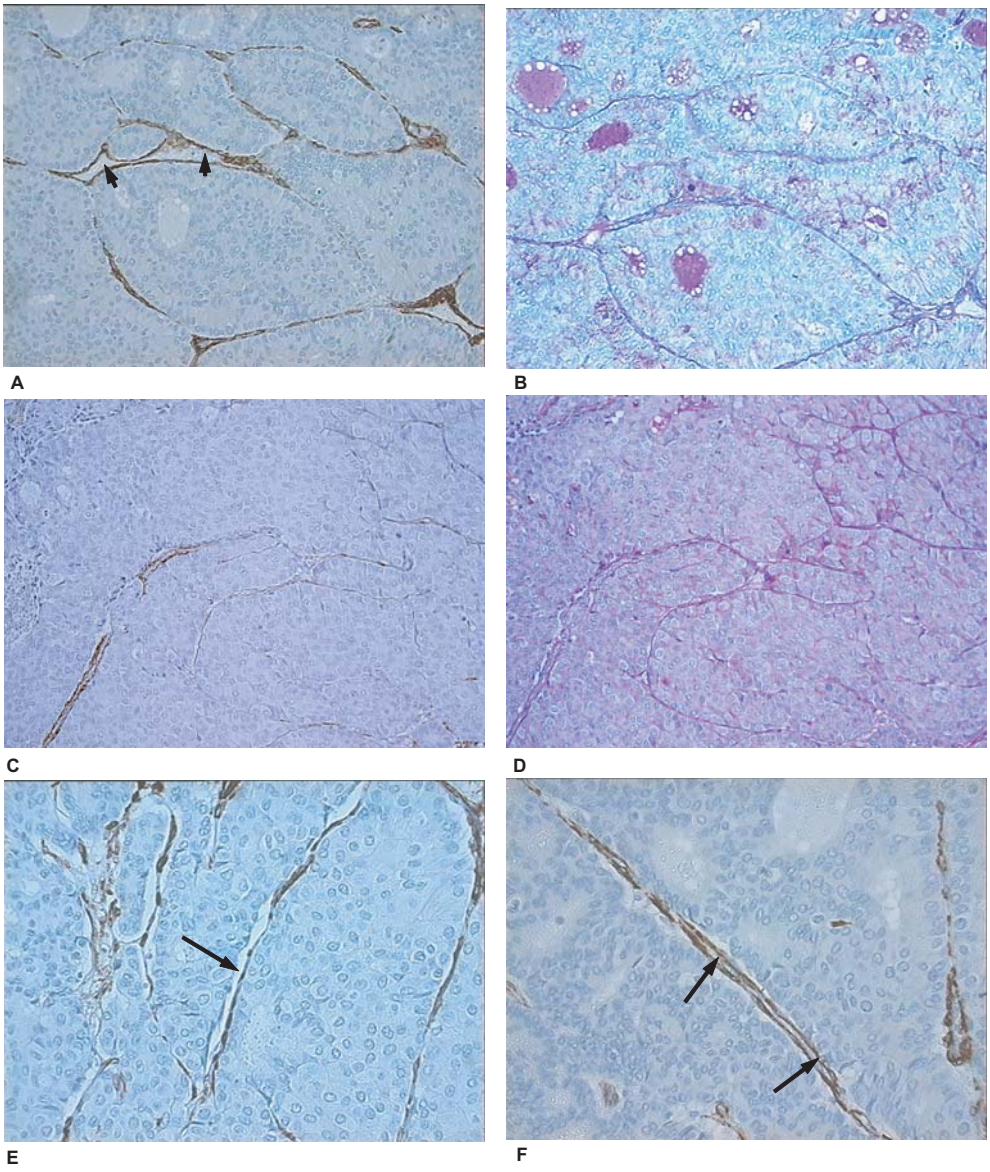

Figure 3 **Expression of Smooth Muscle Actin (SMA)(Compared to a PAS-staining) in a Primary Mammary Carcinoma and Lymph Node Metastasis.** Staining for SMA (*A*, *C*) and the PAS-staining (*B*, *D*) on sequential slides show both the same loops, in primary mamma carcinoma (*A*, *B*) as well as in lymph node metastasis (*C*, *D*). With a higher magnification erythrocytes could be clearly seen (arrowheads, magnification not shown) (magnifications 200x). Both unilateral (*E*) and bilateral (*F*) staining with SMA of the lumen is seen (magnifications 400x).

In contrast, the KM survival curves for patients with positive lymph nodes consisting of PAS+ networks or loops revealed a highly significant shorter period of DFS ($p < 0.0001$ and $p = 0.0002$, respectively) and survival (both p-values < 0.0001) compared to patients lacking these structures (Fig. 5*A,B* and 6*A,B*). All patients with PAS+ arcs or arcs with cross-linking in their positive lymph nodes also had a significant shorter period of DFS ($p = 0.004$ and $p = 0.005$, respectively) and total survival ($p = 0.003$ and $p = 0.0009$) than patients without PAS+ arcs (with cross-linking) (Fig. 5*C,D* and 6*C,D*). There was a trend for patients with lymph node metastases containing PAS+ parallel lanes and PAS+ parallel lanes with cross-linking ($p = 0.07$ and $p = 0.08$, respectively) for a shorter period of DFS (Fig. 5*E,F*). However, the presence of PAS+ parallel lanes (with cross-links) did not give a poor prognosis for total survival (Fig. 6*E,F*). Nevertheless, the presence of any thin PAS+ pattern – including (interconnected) loops, arcs (with branching) and parallel lanes (with cross-links) – in positive lymph nodes is a prognostic indicator for DSF ($p = 0.002$) and, to a lesser extent, for survival ($p = 0.08$) (Fig. 5*G* and 6*G*).

The Cox proportional hazard model using forward selection showed that PAS+ networks in positive lymph nodes and the stage-classification are the two independent risk factors for the occurrence of a distant metastasis (Table 6). Other risk factors were not independently associated with disease free survival, since no other risk factor entered into the Cox model. Furthermore, the presence of a PAS+ networks in positive lymph nodes was the risk factor most strongly associated with poor prognosis.

Discussion

We demonstrate here that, in addition to the tumor blood vessels, different thin PAS+ meshworks may exist in primary breast carcinomas and their lymph node metastases. These PAS+ meshworks are characterized by continuous expression of SMA and patchy expression of CD31. Within these PAS+ meshworks Flt-4+ and vWF+ vessels are embedded.

More importantly, we found that prognosis of clinical outcome is inversely related to the complexity of the PAS+ meshwork in lymph node metastases. Furthermore, the presence of the most complex PAS+ pattern, the PAS+ network, in lymph node metastases from invasive ductal carcinoma of the breast and stage classification of the tumor are the only two independent risk factors associated with the occurrence of a distant metastasis. The presence of a PAS+ network in a positive lymph node is the factor most strongly associated with poor prognosis. In line with previously published studies comparing overall survival and disease free survival in patients that received MRM and BCT as original treatment, the type of treatment was not an independent risk factor for poor prognosis [22-24]. The histological grade was not an independent risk factor, since patients selected in the study had at least one lymph node metastasis and there was, therefore, a bias for a high histological grade. Similarly, the number of positive lymph nodes was not an independent risk factor, since it already entered in the model with the variable stage classification.

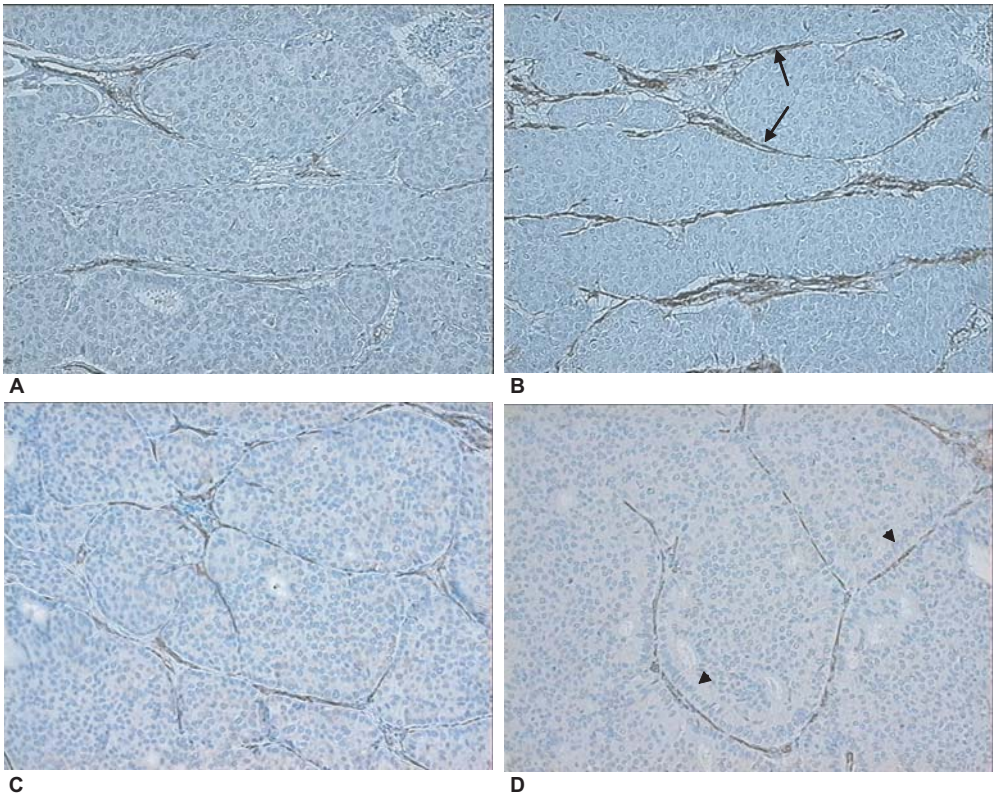

Figure 4 **Expression of CD31 and SMA in Lymph Node Metastasis from a Primary Mammary Carcinoma.** The staining for CD31 (*A*) and SMA (*B*) on sequential slides show co-expression on blood vessels. Additionally, SMA-positive (SMA+) lumina could be seen (arrows). The CD31-positive (CD31+) vessels seems to be connected to each other by the (lumina of) SMA+ framework. *C*, occasionally, however, CD31+ patterns are present alongside the SMA-positive/PAS-positive (SMA+/PAS+) framework. *D*, CD31+ patterns alongside the SMA+/PAS+ framework are also present in the primary mammary carcinoma. Sometimes, breast cancer cells are ordered to the SMA+/PAS+ framework (arrowheads), resembling the manner of normal breast ductal epithelial cells that are polarized to myoepithelium (all magnifications 200x).

Immunohistochemically, these PAS+ meshworks showed continuous expression of SMA (normally expressed by pericytes) and patchy expression of CD31. The presence of lumina in the PAS+ meshwork might be indicative for septa that may facilitate perfusion and/or dissemination of cancer cells. Indeed, tumor cells were frequently present in the lumina, whereas, erythrocytes were occasionally found in these structures.

In 63 % of the patients thin PAS+ patterns were present in both the primary tumors and in their respective lymph nodes. Some tumors may, therefore, have the capability to form such PAS+ patterns, however, none of the PAS+ patterns scored in primary tumors appeared to be of prognostic significance. The non-prognostic value of PAS+ networks in primary

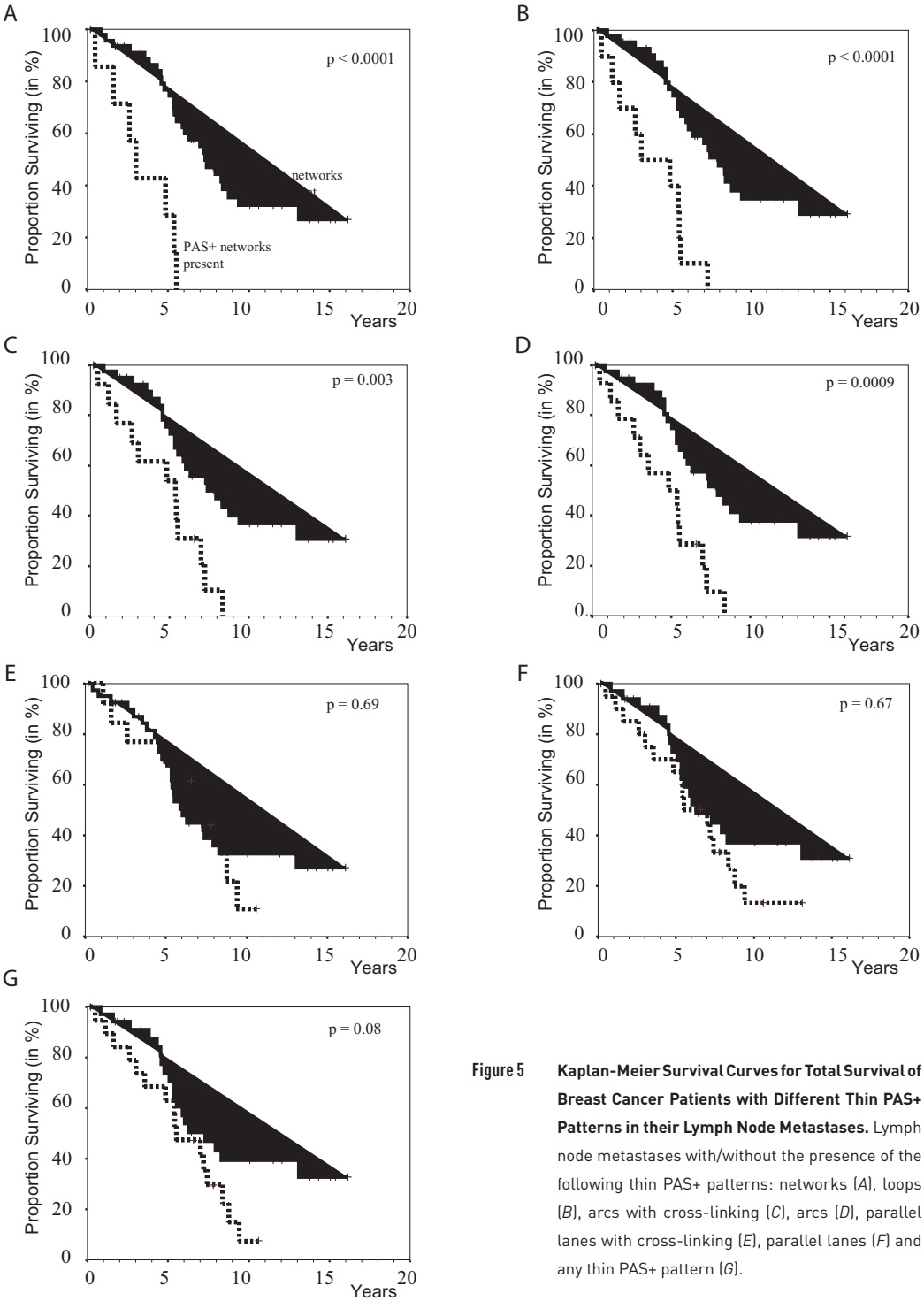

Figure 5 **Kaplan-Meier Survival Curves for Total Survival of Breast Cancer Patients with Different Thin PAS+ Patterns in their Lymph Node Metastases.** Lymph node metastases with/without the presence of the following thin PAS+ patterns: networks (*A*), loops (*B*), arcs with cross-linking (*C*), arcs (*D*), parallel lanes with cross-linking (*E*), parallel lanes (*F*) and any thin PAS+ pattern (*G*).

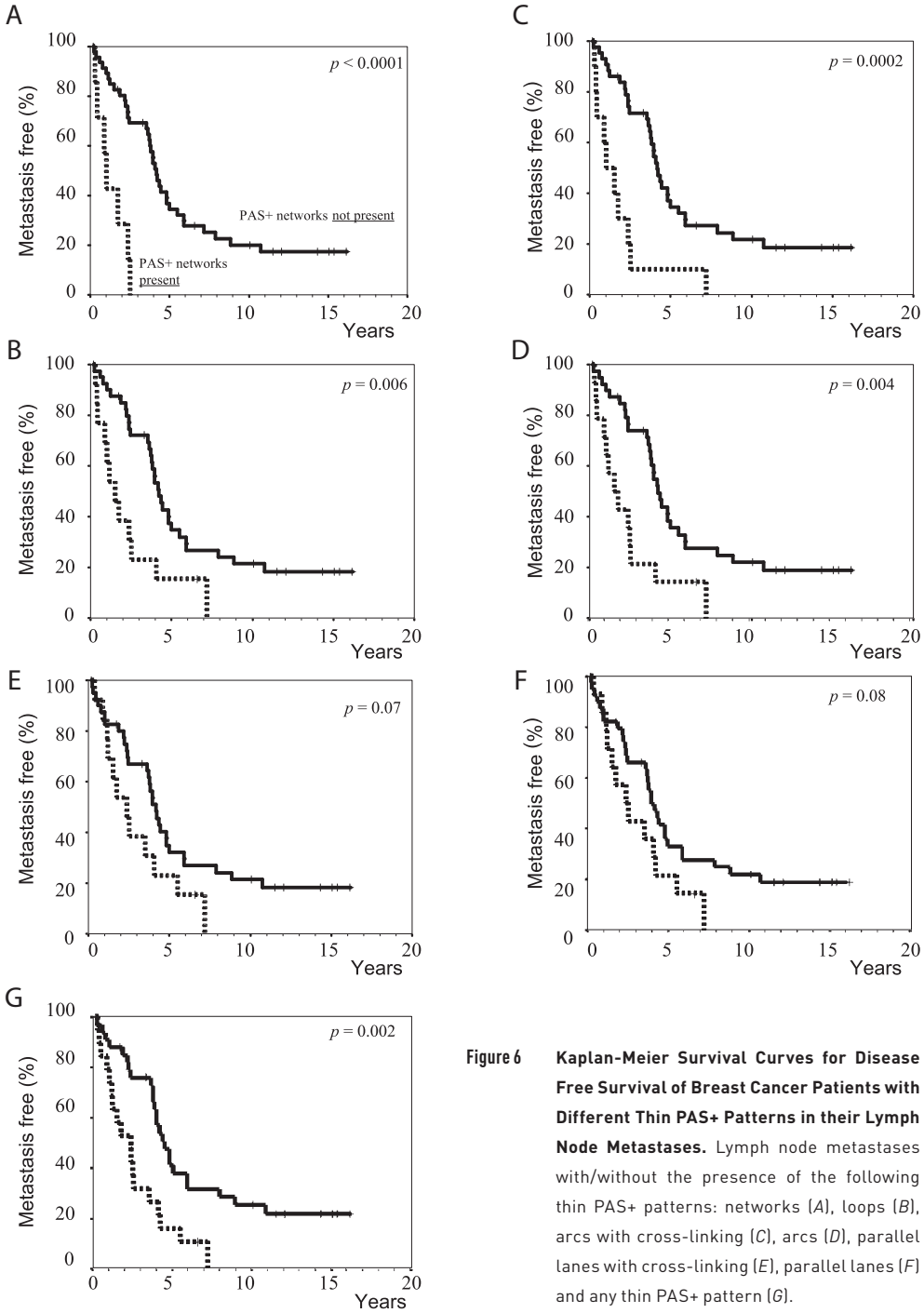

Figure 6 **Kaplan-Meier Survival Curves for Disease Free Survival of Breast Cancer Patients with Different Thin PAS+ Patterns in their Lymph Node Metastases.** Lymph node metastases with/without the presence of the following thin PAS+ patterns: networks (*A*), loops (*B*), arcs with cross-linking (*C*), arcs (*D*), parallel lanes with cross-linking (*E*), parallel lanes (*F*) and any thin PAS+ pattern (*G*).

tumors can be explained by the co-existence of other PAS+/SMA+ structures in primary tumors or normal breast tissue, that hamper the interpretation. Most probably, myoepithelial cells and myofibroblasts interfere with scoring of the PAS+ patterns in the primary breast cancer. Other apparent inconsistencies, e.g. the association of PAS+ parallel lanes (with cross-links) in lymph nodes with poor prognosis for DFS, but not for total survival, are most likely due to the relatively small number of cases.

It has been well established that malignant breast cancer cells can acquire a mesenchymal phenotype, and transit into a myofibroblast, a process known as epithelial-to-mesenchymal transition (EMT)[25-27]. It is tempting to speculate that tumor cells that align hollow tubular structures are phenotypically distinct from other tumor cells and acquire a fibroblast-like phenotype. Accordingly, the process of epithelial-mesenchymal transition might be a prerequisite for a tumor to form such a network [28]. The generation of such a PAS+ network by genetically deregulated, aggressive tumor cells was termed 'vasculogenic mimicry' (VM) to emphasize their *de novo* generation without participation of endothelial cells and independent of angiogenesis [16,18,29-33]. In VM, the PAS+ interconnected loops are the tumor-lined vessels providing perfusion of erythrocytes. Recent reports suggest that VM also exists in ovarian [34], prostate [28] and breast cancer [29,35]. After establishing an inflammatory breast cancer (IBC) xenograft with VM features [36], Shirakawa and co-workers examined surgically resected breast cancers and classified 7,9 % as containing VM [35]. The existence of VM increased the likelihood of hematogenous spread and gave a poorer prognosis for the patient. However, in this study, erythrocytes were only occasionally detected within the PAS+ network. The PAS+ network may also consist of the PAS+ fluid-conducting spaces without erythrocytes in the form of stromal sheets between nests of tumor cells that could provide nutrition for the tumor cell, and probably facilitate metastasis [11].

In addition, Foss and co-workers provided evidence that PAS+ extracellular septa could be particularly favorable substrates for the in-growth of angiogenic, and possibly lymphatic, vessels [16]. Consequently, tumors that contain these PAS+ structures might be more aggressive, as these structures provide better means for (blood) vessel in-growth than tumors lacking these structures. The lack of continuous flt-4 expression in the PAS+ networks of breast cancer patients may, therefore, indicate that these structures do not entirely represent lymphatic vasculature. Indeed, the differences in distribution of flt-4+ and CD31+ patterns within the PAS+ networks in our tissue specimens from the patients, supports the notion that PAS+ meshworks are complex and consist of multiple types of vasculature (blood vessels, and possibly lymphatics). If the septa consist of two layers of ECM elaborated by opposing layers of tumor cells, the layers could separate, forming channels and laminar openings. Such openings could particularly lead to capillary growth. The patchy expression of the endothelial marker, CD31, is in agreement with this hypothesis. Finally, it has been suggested that the open ends of the growing capillaries could feed blood into the channels, therefore, the presence of erythrocytes in the channels could be explained, and different hypotheses could be reconciled [37].

In conclusion, we show here that the presence of PAS+ networks in lymph node metastases from invasive ductal carcinoma of the breast is one of the two independent risk factors for the occurrence of distant metastases. Moreover, the presence of a PAS+ network in a positive lymph node is the factor most strongly associated with occurrence of a distant metastasis. Therefore, by examining the presence of PAS+ networks in invasive ductal carcinoma of the breast, clinical behavior of this heterogeneous group of patients can be better predicted leading to early more aggressive management. Further research should focus in elucidating the exact nature and origin of the PAS+ network in different carcinomas. The investigation of the – possibly tumor-derived – PAS+ patterns, as observed in breast cancer, can have pathophysiological and therapeutic implications ranging from predisposition to blood-borne spread of tumor cells, to facilitated entry of drugs into tumors, and to efficacy of anti-cancer drugs as anti-angiogenic agents.

Acknowledgment

The authors thank Ronald Brand from the Dept. of Statistics for his advise and comments on the statistical analyses. This work has been supported by the Dutch Cancer Society (Grant nr. RUL 2001-2485).

References

1. Orr RK. The impact of prophylactic axillary node dissection on breast cancer survival--a Bayesian meta-analysis. *Ann Surg Oncol* 1999; 6:109-16.
2. Folkman J. Angiogenesis in cancer, vascular, rheumatoid and other disease. *Nat Med* 1995; 1:27-31.
3. Risau W. Mechanisms of angiogenesis. *Nature* 1997; 386:671-4.
4. Hanahan D, Folkman J. Patterns and emerging mechanisms of the angiogenic switch during tumorigenesis. *Cell* 1996; 86:353-64.
5. Rak J, Kerbel RS. Treating cancer by inhibiting angiogenesis: new hopes and potential pitfalls. *Cancer Metastasis Rev* 1996; 15:231-6.
6. Kumar R, Fidler IJ. Angiogenic molecules and cancer metastasis. *In Vivo* 1998; 12:27-34.
7. de Jong JS, van Diest PJ, Baak JP. Hot spot microvessel density and the mitotic activity index are strong additional prognostic indicators in invasive breast cancer. *Histopathology* 2000; 36:306-12.
8. Engels K, Fox SB, Harris AL. Angiogenesis as a biologic and prognostic indicator in human breast carcinoma. *EXS* 1997; 79:113-56.:113-56.
9. Gasparini G, Harris AL. Clinical importance of the determination of tumor angiogenesis in breast carcinoma: much more than a new prognostic tool. *J Clin Oncol* 1995; 13:765-82.
10. Harris AL, Zhang H, Moghaddam A, Fox S, Scott P, Pattison A *et al*. Breast cancer angiogenesis--new approaches to therapy via antiangiogenesis, hypoxic activated drugs, and vascular targeting. *Breast Cancer Res Treat* 1996; 38:97-108.
11. Clarijs R, Otte-Holler I, Ruiter DJ, de Waal RM. Presence of a fluid-conducting meshwork in xenografted cutaneous and primary human uveal melanoma. *Invest Ophthalmol Vis Sci* 2002; 43:912-8.
12. Folberg R, Pe'er J, Gruman LM, Woolson RF, Jeng G, Montague PR *et al*. The morphologic characteristics of tumor blood vessels as a marker of tumor progression in primary human uveal melanoma: a matched case-control study. *Hum Pathol* 1992; 23:1298-305.

13. Thies A, Mangold U, Moll I, Schumacher U. PAS-positive loops and networks as a prognostic indicator in cutaneous malignant melanoma. *J Pathol* 2001; 195:537-42.
14. Folberg R, Rummelt V, Parys-Van Ginderdeuren R, Hwang T, Woolson RF, Pe'er J *et al*. The prognostic value of tumor blood vessel morphology in primary uveal melanoma. *Ophthalmology* 1993; 100:1389-98.
15. Warso MA, Maniotis AJ, Chen X, Majumdar D, Patel MK, Shilkaitis A *et al*. Prognostic significance of periodic acid-Schiff-positive patterns in primary cutaneous melanoma. *Clin Cancer Res* 2001; 7:473-7.
16. Foss AJ, Alexander RA, Hungerford JL, Harris AL, Cree IA, Lightman S. Reassessment of the PAS patterns in uveal melanoma. *Br J Ophthalmol* 1997; 81:240-6.
17. McLean IW, Keefe KS, Burnier MN. Uveal melanoma. Comparison of the prognostic value of fibrovascular loops, mean of the ten largest nucleoli, cell type, and tumor size. *Ophthalmology* 1997; 104:777-80.
18. Maniotis AJ, Folberg R, Hess A, Seftor EA, Gardner LM, Pe'er J *et al*. Vascular channel formation by human melanoma cells in vivo and in vitro: vasculogenic mimicry. *Am J Pathol* 1999; 155:739-52.
19. van den Broek LJ, van de Vijver MJ. Assessment of problems in diagnostic and research immunohistochemistry associated with epitope instability in stored paraffin sections. *Appl Immunohistochem Molecul Morphol* 2000; 8:316-21.
20. Hazelbag HM, van den Broek LJ, van Dorst EB, Offerhaus GJ, Fleuren GJ, Hogendoorn PC. Immunostaining of chain-specific keratins on formalin-fixed, paraffin-embedded tissues: a comparison of various antigen retrieval systems using microwave heating and proteolytic pre-treatments. *J Histochem Cytochem* 1995; 43:429-37.
21. Valtola R, Salven P, Heikkila P, Taipale J, Joensuu H, Rehn M *et al*. VEGFR-3 and its ligand VEGF-C are associated with angiogenesis in breast cancer. *Am J Pathol* 1999; 154:1381-90.
22. Lee HD, Yoon DS, Koo JY, Suh CO, Jung WH, Oh KK. Breast conserving therapy in stage I & II breast cancer in Korea. *Breast Cancer Res Treat* 1997; 44:193-9.
23. Noguchi M, Yagasaki R, Kawahara F, Minami M, Tsuyama H, Earashi M *et al*. Breast conserving treatment versus modified radical mastectomy in Japanese patients with operable breast cancer. *Int Surg* 1997; 82:289-94.
24. van Tienhoven G, Voogd AC, Peterse JL, Nielsen M, Andersen KW, Mignolet F *et al*. Prognosis after treatment for loco-regional recurrence after mastectomy or breast conserving therapy in two randomised trials (EORTC 10801 and DBCG-82TM). EORTC Breast Cancer Cooperative Group and the Danish Breast Cancer Cooperative Group. *Eur J Cancer* 1999; 35:32-8.
25. Petersen OW, Lind NH, Gudjonsson T, Villadsen R, Ronnov-Jessen L, Bissell MJ. The plasticity of human breast carcinoma cells is more than epithelial to mesenchymal conversion. *Breast Cancer Res* 2001; 3:213-7.
26. Thiery JP. Epithelial-mesenchymal transitions in tumour progression. *Nat Rev Cancer* 2002; 2:442-54.
27. Dandachi N, Hauser-Kronberger C, More E, Wiesener B, Hacker GW, Dietze O *et al*. Co-expression of tenascin-C and vimentin in human breast cancer cells indicates phenotypic transdifferentiation during tumour progression: correlation with histopathological parameters, hormone receptors, and oncoproteins. *J Pathol* 2001; 193:181-9.
28. Sharma N, Seftor RE, Seftor EA, Gruman LM, Heidger PM, Jr., Cohen MB *et al*. Prostatic tumor cell plasticity involves cooperative interactions of distinct phenotypic subpopulations: Role in vasculogenic mimicry. *Prostate* 2002; 50:189-201.
29. Hendrix MJ, Seftor EA, Kirschmann DA, Seftor RE. Molecular biology of breast cancer metastasis. Molecular expression of vascular markers by aggressive breast cancer cells. *Breast Cancer Res* 2000; 2:417-22.
30. McDonald DM, Munn L, Jain RK. Vasculogenic mimicry: how convincing, how novel, and how significant? *Am J Pathol* 2000; 156:383-8.
31. Folberg R, Hendrix MJ, Maniotis AJ. Vasculogenic mimicry and tumor angiogenesis. *Am J Pathol* 2000; 156:361-81.
32. Fausto N. Vasculogenic mimicry in tumors. Fact or artifact? *Am J Pathol* 2000; 156:359.
33. Bissell MJ. Tumor plasticity allows vasculogenic mimicry, a novel form of angiogenic switch. A rose by any other name? *Am J Pathol* 1999; 155:675-9.

34. Sood AK, Seftor EA, Fletcher MS, Gardner LM, Heidger PM, Buller RE *et al*. Molecular determinants of ovarian cancer plasticity. *Am J Pathol* 2001; 158:1279-88.
35. Shirakawa K, Wakasugi H, Heike Y, Watanabe I, Yamada S, Saito K *et al*. Vasculogenic mimicry and pseudo-comedo formation in breast cancer. *Int J Cancer* 2002; 99:821-8.
36. Shirakawa K, Tsuda H, Heike Y, Kato K, Asada R, Inomata M *et al*. Absence of endothelial cells, central necrosis, and fibrosis are associated with aggressive inflammatory breast cancer. *Cancer Res* 2001; 61:445-51.
37. Ruoslahti E. Specialization of tumour vasculature. *Nature Cancer Reviews* 2002; 2:83-90.